Mechatronics 19 (2009) 1169–1177

Contents lists available at ScienceDirect

Mechatronics

journal homepage: www.elsevier.com/locate/mechatronics

Modeling, control and experimental validation of a novel actuator based on shape memory alloys

Roberto Romano [a], Eduardo Aoun Tannuri [b,*]

[a] Instituto de Pesquisas Tecnológicas do Estado de São Paulo, São Paulo, Brazil
[b] Mechatronics Engineering Department, Escola Politécnica da Universidade de São Paulo, São Paulo, Brazil

ARTICLE INFO

Article history:
Received 19 May 2008
Accepted 22 March 2009

Keywords:
Modeling
Shape memory alloy
Actuator
Robotics
Sliding mode control

ABSTRACT

The paper presents the development of a mechanical actuator using a shape memory alloy with a cooling system based on the thermoelectric effect (Seebeck–Peltier effect). Such a method has the advantage of reduced weight and requires a simpler control strategy as compared to other forced cooling systems. A complete mathematical model of the actuator was derived, and an experimental prototype was implemented. Several experiments are used to validate the model and to identify all parameters. A robust and nonlinear controller, based on sliding-mode theory, was derived and implemented. Experiments were used to evaluate the actuator closed-loop performance, stability, and robustness properties. The results showed that the proposed cooling system and controller are able to improve the dynamic response of the actuator.

1. Introduction

Shape Memory Alloys (SMAs) consist of a group of metallic materials that demonstrate the ability to return to some previously defined shape or size when subjected to the appropriate thermal procedure. The shape memory effect occurs due to a temperature and stress dependent shift in the materials crystalline structure between two different phases called Martensite and Austenite. Martensite, the low temperature phase, is relatively soft whereas Austenite, the high temperature phase, is relatively hard. The change that occurs within SMAs crystalline structure is not a thermodynamically reversible process and results in temperature hysteresis. SMAs have been used in a variety of actuation applications. The key feature of this material is its ability to undergo seemingly large strains in the Martensite phase and subsequently recover these strains when the material is heated and the phase transformation to Austenite occurs. SMA actuators have several advantages such as excellent power-to-mass ratio, maintainability, reliability, and clean and silent actuation. The disadvantages are low energy efficiency due to conversion of heat to mechanical energy, inaccurate motion control due to hysteresis, nonlinearities, parameter uncertainties, difficulty in measuring variables such as temperature, and slow response due to the thermal process involved in the working principle.

To operate quickly and to obtain a good dynamic performance, the SMA must be cooled and heated rapidly. The heating process is usually based on the Joule effect, using electric current along the SMA element. Such a method is very fast, and may be easily controlled by standard electronic circuits. However, the cooling process evolves heat transfer phenomena that are normally slow and very difficult to control.

Some researchers have proposed static cooling methods, in which the SMA wires are continually cooled by means of an air stream [17]. In a similar way, Furuya and Shimada [8] used a cooling system based on water immersion. In such a case, cooling time was reduced by 10 times compared to a non-cooled wire. Asada and Mascaro [2] developed an actuator with a cooling system based on flowing water around the wire. A complex system guarantees that water flows only when wire must be cooled. The dynamic response of the actuator is expressively better.

The main drawbacks of such actuators are related to the complexity of the cooling systems that require pumps or compressors with sealing systems. They also increase the total power consumption of the actuators, up to a factor of 20, since in the heating phase it is necessary to use much more power to compensate for the heat that is lost by the cooling system.

Another approach was proposed by Gorbet and Russel [9], using passive components to cool the wire. The authors used a mobile metallic heat sink and a mechanism which guaranteed that the sink was only in contact with the wire being cooled, which minimizes the power consumption of the actuator and increases its dynamic behavior. The main drawback of that system is the complex mechanism, based on a mechanical clutch exposed to continuous wear, which reduces the life time and the robustness of the actuator.

* Corresponding author. Tel./fax: +551130915414.
E-mail address: eduat@usp.br (E.A. Tannuri).

0957-4158/$ - see front matter © 2009 Elsevier Ltd. All rights reserved.
doi:10.1016/j.mechatronics.2009.03.007

Nomenclature

A	external area per unity length, m^2/m
A_s, A_f	initial and final temperature of austenite transformation
A_{wire}	sectional area of the wire, m^2
c	damping coefficient, Ns/m
C	conduction coefficient, W/°C/m
c_P	specific heat, J/kg K
d	diameter of the wire, m
E	Young's Modulus, N/m^2
h	natural convection coefficient, W/m^2 °C/m
i	electric current in the wire, A
I	total inertia, kg
J	moment of inertia of the pulley, kg m^2
K	equivalent stiffness coefficient of the wire, N/m
K_{SM}	sliding mode control gain
m	mass per unity length, kg/m
m_L	mass of the load, kg
M_s, M_f	initial and final temperature of martensite transformation
n	motion amplification factor
R	electrical resistance per unity length, Ω/m
r_1,r_2	internal and external pulley radius, m
T	SMA wire temperature, °C
T_1, T_2	force (traction), N
T_p	temperature on the surface of the cooling element, °C
T_{amb}	ambient temperature, °C
x	load position, m

Greek symbols

Δ	maximum wire elongation, m
ε	deformation (strain) of the wire
ε_{my}	martensite maximum elastic deformation
λ	sliding mode control parameter
ξ	martensite fraction (0–100%)
ξ_m	highest martensite fraction during cooling
ξ_A	initial value of martensite fraction during cooling
ϕ	boundary layer thickness
σ	mechanical stress in the wire, N/m^2
ω	angular velocity of the pulley, rad/s

Subscripts

A	relative to austenite
M	relative to martensite

Other authors have used thermoelectric effect (Seebeck–Peltier effect) in order to improve the dynamic performance of SMA actuators. For example, Semenyuk et al. [15] and Khan et al. [14] developed SMA actuators in which the thermoelectric cooler is separated from SMA wire. Heat is extracted from the wire by thermal conduction. Bhattacharyya et al. [3], Ding and Lagoudas [4] and Abadie et al. [1] have proposed a different approach, with a maximal integration of the thermoelectric phenomenon. In this case, the thermoelectric connections are directly made on the SMA element, and better dynamic performance has been reported. However, more complex manufacturing of the SMA wire integrated with the thermoelectric element is required.

The present paper proposes a similar approach of thermoelectric cooler separated from SMA wire, due to the simplicity of the solution and the possibility of using commercial thermoelectric tablets. The thermoelectric tablet is constantly powered and keeps the low temperature on its cold face that is in permanent contact with the SMA wire. A heat sink is used to dissipate the generated heat. The proposed cooling system presents a simple mechanical design, with no moving parts or sophisticated mechanisms. Furthermore, it does not require complex accessories like pumps or compressors, and the manufacturing/assembly of the SMA wire and thermoelectric tablet requires no special process.

A drawback of the present proposal is that the wire is continually cooled by the thermoelectric tablet, even when it is heated by the electric current, due to the poor dynamic performance of the commercial thermoelectric tablet. Such a fact results in larger power consumption, but does not affect the dynamic performance, as will be shown later. In order to obtain a good dynamic performance, a full-nonlinear and robust sliding mode control, based on the model of the actuator, was then derived. It has been demonstrated that such a controller compensated for the mentioned drawbacks, and an acceptable dynamic performance of the actuator has been obtained.

In the present work, a complete mathematical model of the actuator was derived and an experimental prototype was used to validate the model and identify all parameters. Since the system presents hysteretic behavior and strong nonlinearities, a sliding mode control was then derived and used to control the electric current along the SMA wire. A full set of experiments was then carried out in order to evaluate the dynamic performance of the actuator and to show the advantages of the proposed cooling system and controller.

2. Experimental set-up

An experimental prototype of the SMA actuator, cooled by a thermoelectric element, was built. It was used to validate the mathematical model and to evaluate the control algorithm. Fig. 1 shows a simple scheme of the actuator. A 15 × 5 cm thermoelectric tablet is assembled in a heat sink and a small blower is also used to dissipate the heat. The SMA wire is attached to the structure by means of an electric connector C_1. The other end of the wire is attached to the internal pulley (radius r_1 = 0.45 cm). A 40 g load is supported by a wire connected to the external pulley (r_2 = 4.5 cm). The length of the SMA wire is 15 cm, and its typical 4.0% deformation is amplified by a factor $n = r_2/r_1 \cong 10$. So, what is expected is a 6 cm elevation of the load, which is equivalent to

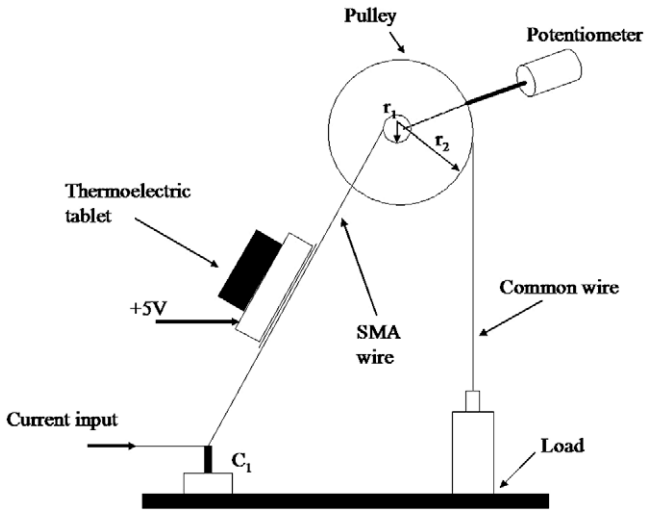

Fig. 1. Diagram of the SMA actuator.

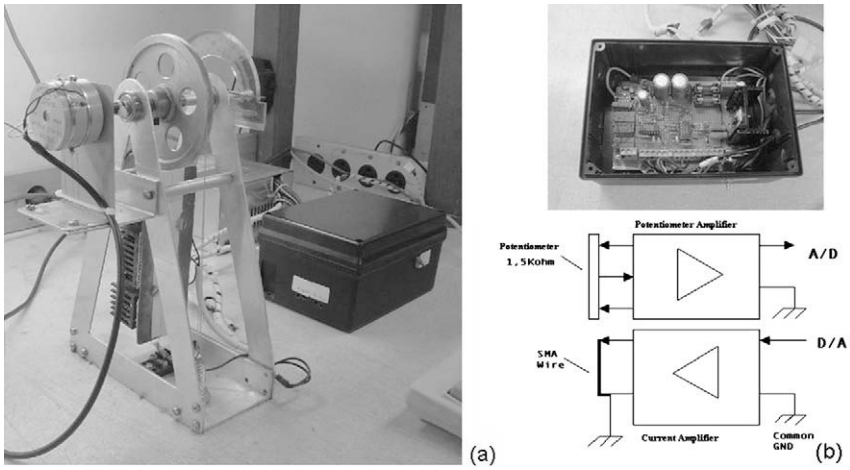

Fig. 2. (a) Picture of the actuator ; (b) Picture and diagram of the signal conditioning module.

a 76° pulley rotation. Such a rotation is measured by a potentiometer directly attached to the pulley axis.

Fig. 2a shows a picture of the actuator. The signal conditioning module is shown in Fig. 2b. It is composed of a constant current amplifier that supplies up to 1 A electric current to heat the SMA wire, and by a voltage amplifier/filter connected to the potentiometer. The module is connected to a computer (Pentium 100 MHz) by means of a 10-bit AD/DA board. The thermoelectric tablet is constantly powered by a 5 V electric source.

Matlab/Simulink software was used to acquire and process the data from the potentiometer, and to send the command for the current that must be imposed on the SMA wire. Such software is flexible, and several control algorithms can be easily implemented. Furthermore, all graphical and mathematical tools provided by Matlab/Simulink can be used. The interface with AD/DA board was developed by means of low-level code included in the software. Fig. 3 shows a picture of the whole system.

3. Mathematical model

The model developed in the present work is based on the formulations proposed by Ikuta et al. [12], Grant et al. [10], Elahinia and Ashrafiuon [7], Hoder et al. [11] and Dutta and Ghorbel [5]. It is composed of a thermal model, a phase transformation model, and a description of the mechanical properties and dynamics of the system (Fig. 4).

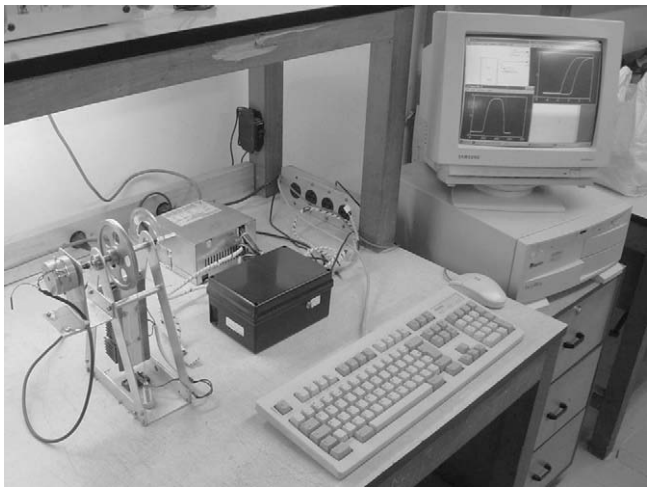

Fig. 3. SMA actuator and controlling computer.

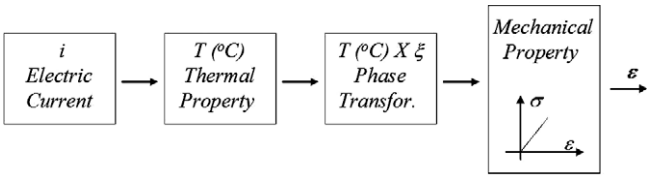

Fig. 4. SMA actuator model.

3.1. Thermal model

The thermal model was based on the system shown in Fig. 5, in which the SMA wire touches the thermoelectric element. The temperature of the element is considered to be constant and equal to 15 °C.

Considering several simplification hypotheses [10], the thermal model can be written as (thermomechanical coupling is also not included since the deformation rate of the SMA wire is small, and such an effect becomes important for fast or highly oscillatory deformations):

$$m \cdot c_p \cdot \frac{dT}{dt} = i^2 \cdot R - h \cdot A \cdot (T - T_{amb}) - C \cdot (T - T_p) \quad (1)$$

The temperature T_p on the surface of the cooling element is 15°C and T_{amb} is the ambient temperature, considered to be 24 °C. The electric current i is the main control variable of the system.

Technical specifications of the SMA wire (Flexinol FLX 00870, 0.008'', 70 °C) are listed in Dynalloy [6], and are given by:

$m - 2.10^{-4}$ kg/m; $c_p - 837$ J/kg K; $R - 32\ \Omega$/m; $A - 6.28.10^{-4}$ m^2/m; $d - 2.10^{-4}$ m

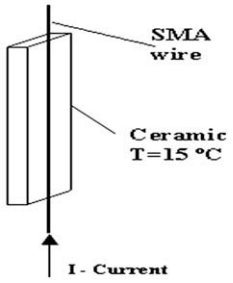

Fig. 5. SMA wire and cooling element.

The parameters h and C are very difficult to estimate, since they depend on several variables. A rough estimation of such parameters, based on the theory included in Incropera and Witt [13], are $C = 0.4$ W/°C/m and $h = 6.55$ W/m^2°C/m. In the sequel, an identification procedure will be used to obtain values closer to the real ones.

The thermoelectric tablet presents a slow dynamic response, with a settling time of approximately 60 s for cooling and more than 160 s for heating. Fig. 6 shows the step response of the tablet, after applying a constant 5 V voltage at $t = 0$ s and turning it off at $t = 110$ s.

Due to such a slow response, the T_p temperature may not be used as an extra control variable, since the actuator presents a settling time smaller than 1 s. Therefore, it was decided to keep the thermoelectric tablet constantly powered, and thus its effect in the system will be to reduce the temperature around the wire, decreasing the cooling time when the electric current is switched off. As a result, in the mathematical model, the temperature T_p was considered constant.

3.2. Phase transformation

During heating, the transformation occurs from Martensite (M) to Austenite (A), and during the cooling phase, the opposite transformation occurs. Basic equations that model such transformations as a function of temperature are given below [12]:

$$\begin{aligned}\xi &= \frac{\xi_M}{1+\exp\left[\frac{6.2}{A_f-A_s}\left(T-\frac{A_s+A_f}{2}\right)\right]}(\text{heating});\\ \xi &= \frac{1-\xi_A}{1+\exp\left[\frac{6.2}{M_f-M_s}\left(T-\frac{M_s+M_f}{2}\right)\right]}+\xi_A(\text{cooling})\end{aligned} \tag{2}$$

where A_s and A_f are the initial and final temperature of austenite transformation, respectively; M_s and M_f are the initial and final temperature of martensite transformation, respectively, ξ_M is the highest martensite fraction during cooling, and ξ_A is the initial value of martensite fraction during cooling. Typical values are $A_s = 68$ °C, $A_f = 78$ °C, $M_s = 52$ °C, and $M_f = 42$ °C [6]. However, such values may present variations up to ±15 °C, and an identification procedure will be applied to evaluate the correct values for the wire used in the experimental actuator. A plot of the phase transformation is showed in Fig. 7, and the hysteresis is evident [11],

3.3. Mechanical properties and dynamics

Mechanical properties of shape memory alloys are obtained by means of a multiple layer model. The austenite phase is characterized by an elastic behavior. The martensite phase presents a behavior that seems to be plastic and deformed by a small stress [12]. So, for $\xi = 0$ (full austenite), the stress–strain relation is given by:

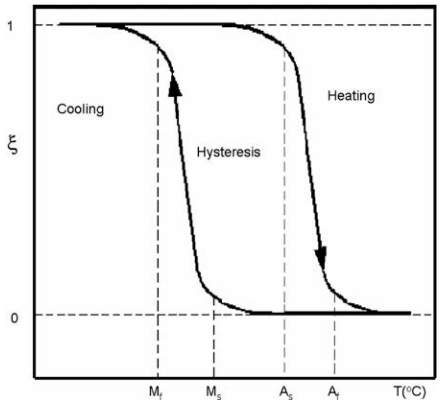

Fig. 7. Phase transformation plot.

$$\sigma_A = E_A \cdot \varepsilon \tag{3}$$

where σ_A is the mechanical stress in the austenite portion of the alloy and E_A is the austenite Young's Modulus. In the opposite way, when $\xi = 1$ (full martensite), the stress–strain relation is given by:

$$\begin{aligned}\sigma_M &= E_M \cdot \varepsilon \quad \text{if } |\varepsilon| \leqslant |\varepsilon_{My}|\\ \sigma_M &= E_M \cdot \varepsilon_{My} \quad \text{if } |\varepsilon| > |\varepsilon_{My}|\end{aligned} \tag{4}$$

where E_M is the martensite Young's Modulus , ε_{My} is the martensite maximum elastic deformation, and σ_M is the maximum stress in the martensite. The martensite mechanical behavior is illustrated in the Fig. 8:

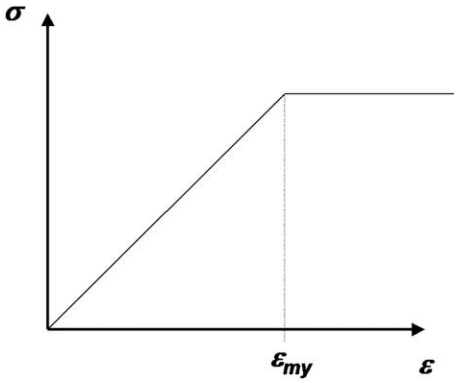

Fig. 8. Martensite mechanical behavior.

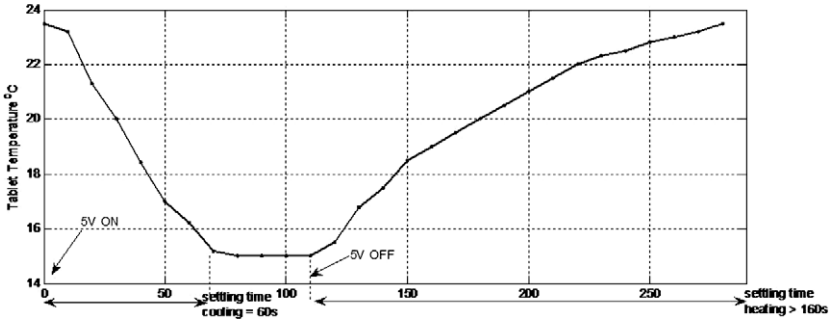

Fig. 6. Step response of the thermoelectric tablet.

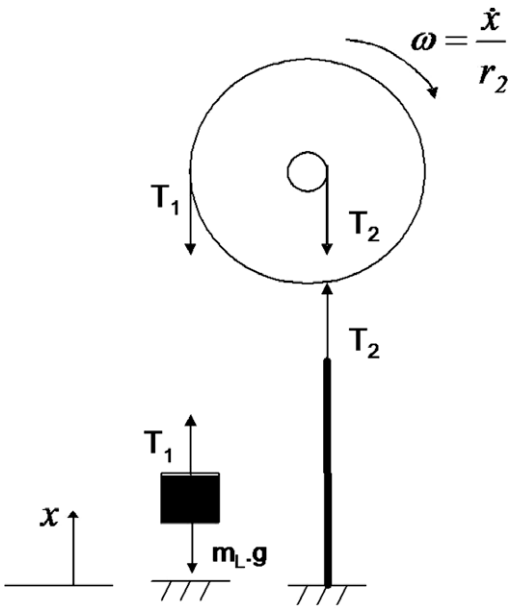

Fig. 9. Diagram of the actuator and main forces.

Considering then the case with $0 < \xi < 1$, the stress–strain relation is given by:

$$\sigma = \xi \cdot \sigma_M + (1-\xi)\cdot\sigma_A \Rightarrow \begin{cases} \varepsilon = \frac{\sigma}{\xi \cdot E_M + (1-\xi)\cdot E_A} & \text{for } |\varepsilon| \leqslant |\varepsilon_{My}| \\ \varepsilon = \frac{\sigma - \xi . E_M . \varepsilon_{My}}{(1-\xi)\cdot E_A} & \text{for } |\varepsilon| > |\varepsilon_{My}| \end{cases} \quad (5)$$

The dynamics of the actuator are now considered. A simplified diagram of the actuator and the main forces are shown in the Fig. 9, where the coordinate x represents the position of the load:

The traction T_1 holds the load, T_2 is the force (traction) acting on the SMA wire, and ω is the angular velocity of the pulley. So, with J being the moment of inertia of the pulley and m_L the mass of the load, using the basic laws of mechanics one obtains:

$$-T_1.r_2 + T_2 r_1 = J \cdot \frac{\ddot{x}}{r_2}; \quad -m_L g + T_1 = m_L \ddot{x} \quad (6)$$

Traction T_2 may be estimated using a linear spring analogy. Fig. 10 shows the wire in three possible states. In the austenite phase, the "spring" presents its initial length l_0. In the martensite phase, the

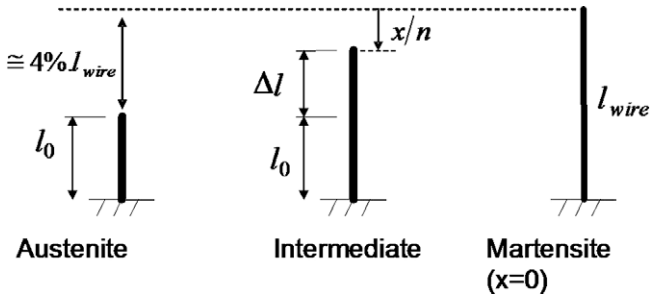

Fig. 10. Spring analogy.

wire reaches its maximum length l_{wire}, that corresponds to the situation in which the load position is $x = 0$. The difference between l_0 and l_{wire} is approximately 4% of the l_{wire}. In an intermediate phase, the "spring" elongation Δl is given by $0.04l_{fio} - x/n$.

The SMA wire traction is given by T_2 $K{\cdot}\Delta l = K(0.04l_{wire} - x/n)$, where K is the equivalent stiffness coefficient of the wire. Including a damping term, the equation of motion of the actuator becomes:

$$(J/r_2^2 + m_L)\cdot\ddot{x} + c\cdot\dot{x} + K/n^2 \cdot x = -m_L g + (0.04 l_{wire} K)/n \quad (7)$$

The stiffness coefficient K may be evaluated using (5). Assuming elastic behavior, and A_{wire} being the sectional area of the wire, one obtains:

$$\sigma = [\xi \cdot E_M + (1-\xi)\cdot E_A].\varepsilon \quad \text{or} \quad \frac{T_2}{A_{wire}} = [\xi \cdot E_M + (1-\xi)\cdot E_A]\cdot\frac{\Delta l}{l_0} \quad (8)$$

Finally, considering that martensite stress will be higher than its elastic limit, it may be assumed that it will present full plastic behavior, with a very small stiffness. So, E_M may be excluded from (8), resulting in the approximation:

$$K = [(1-\xi)\cdot E_A]\cdot\frac{A_{wire}}{l_0} \quad (9)$$

3.4. Parameter identification

Thermal parameters C and h, as well as the transformation temperatures (M_s, M_f, A_s, and A_f) must be accurately evaluated using a proper experimental procedure. A ramp excitation was induced in the wire, inducing a displacement of the load, as shown in Fig. 11.

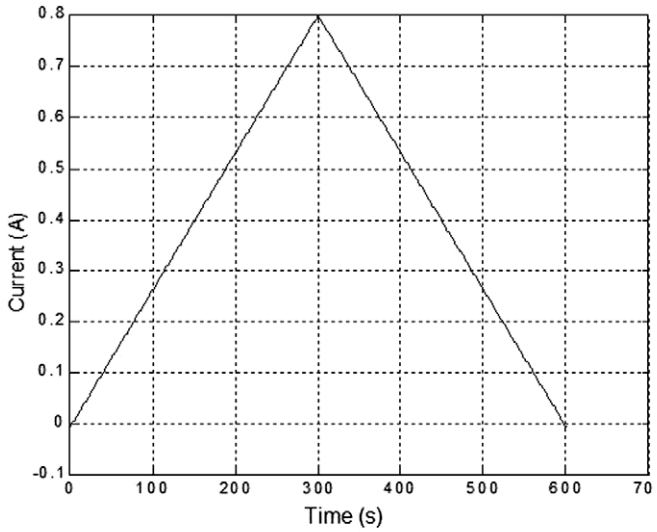

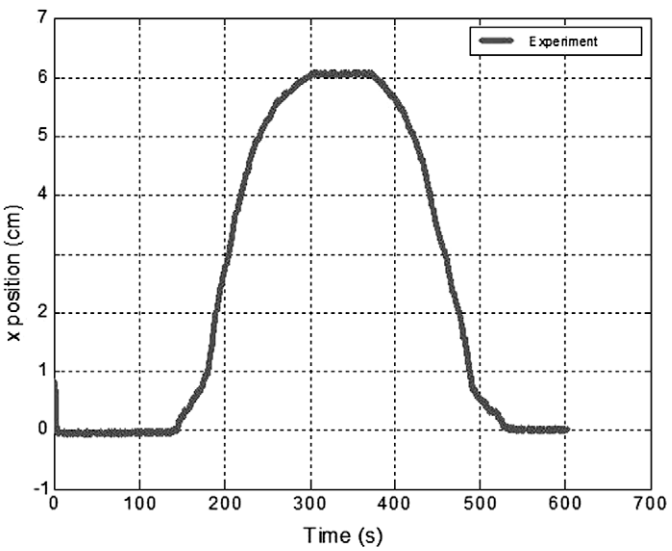

Fig. 11. (left) Current ramp excitation; (right) Position of the load.

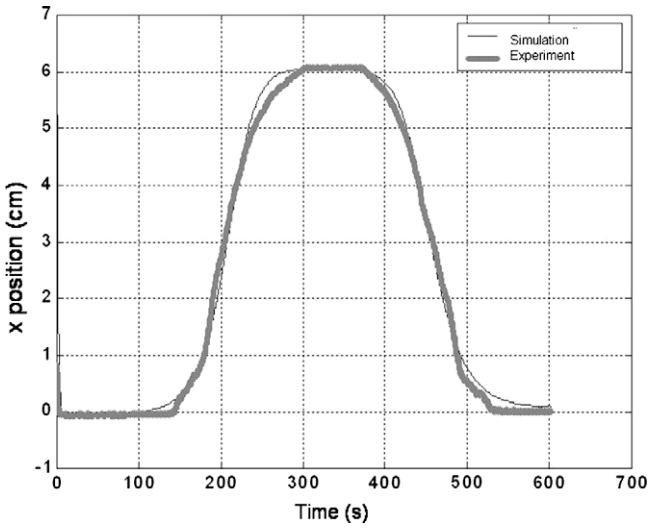

Fig. 12. Comparison between simulation and experimental results.

Using an optimization algorithm based on Quadratic Sequential Programming (SQP), the model parameters were adjusted in order to make the model recover the measured position accurately. The following parameters were obtained: $C = 0.255$ W/°C/m, $h = 7$ W/m²°C/m, $M_s = 66$°C , $M_f = 34$ °C, $A_s = 53$ °C, and $A_f = 93$ °C. The comparison between the measured position and that obtained by the model simulation is given in Fig. 12. Good accuracy of the model can be assured.

4. Control system design

In order to apply the sliding mode control to the SMA actuator, the previously developed model must be adapted following the formulation exposed in Slotine and Li [16]. After some algebraic manipulation using (1) and (2), the dynamics of phase transformation can be written as:

$$\dot{\xi} = f_\xi(\xi) + b_\xi(\xi)\cdot u \tag{10}$$

with:

$$f_\xi(\xi) = \frac{-\alpha}{\xi_0 mc_P}(\xi_0(\xi-k)-(\xi-k)^2) \times \left(hAT_{amb} + CT_P - (hA+C)\left(\frac{1}{\alpha}\ln\left(\frac{\xi_0}{\xi-k}-1\right)+\beta\right)\right)$$

$$b_\xi(\xi) = \frac{-\alpha}{\xi_0 mc_P}(\xi_0(\xi-k)-(\xi-k)^2)R; \quad u = i^2 \quad \text{and}$$

$$\begin{cases} \alpha = \frac{6.2}{A_f - A_s};\ \beta = \frac{A_s + A_f}{2};\ \xi_0 = \xi_M;\ k = 0 & \text{if } \dot{T} > 0 \\ \alpha = \frac{6.2}{M_s - M_f};\ \beta = \frac{M_s + M_f}{2};\ \xi_0 = 1 - \xi_A;\ k = \xi_A & \text{if } \dot{T} < 0 \end{cases}$$

Using (7) and (9), the dynamics of the motion can also be written as:

$$I\ddot{x} + c\dot{x} + \frac{K_0(1-\xi)}{n^2}x = -m_L g + \frac{K_0(1-\xi)}{n}\Delta \tag{11}$$

with $I=(J/r_2^2 + m_L)$; $K_0 = E_A A_{wire}/l_0$ and $\Delta = 0.04 l_{wire}$. In Eqs. (10) and (11), the variable x is measured, but the variable ξ must be estimated. This may be done considering a quasi-static approximation to (11), making $\dot{x} = \ddot{x} = 0$, that results:

$$\hat{\xi} = 1 - \frac{m_L g}{K_0\left(\frac{\Delta}{n} - \frac{x}{n^2}\right)} \tag{12}$$

Differentiating (11) once, and using (10), one obtains the SMA model adequate to apply the sliding mode control, as proposed by Slotine and Li [16]:

$$\dddot{x} = f(\mathbf{x}) + b(\mathbf{x})\cdot u \tag{13}$$

with $\mathbf{x} = (\xi \quad x \quad \dot{x} \quad \ddot{x})^T$,

$$f(\mathbf{x}) = \frac{-c}{I}\ddot{x} - \frac{K_0(1-\xi)}{In^2}\dot{x} + \left(\frac{K_0 x}{In^2} - \frac{K_0\Delta}{In}\right)f_\xi(\xi) \quad \text{and}$$

$$b(\mathbf{x}) = \left(\frac{K_0 x}{In^2} - \frac{K_0\Delta}{In}\right)b_\xi(\xi)$$

So, the control action $u = i^2$ is given by:

$$u = \frac{1}{\hat{b}(\mathbf{x})}\left(-\hat{f}(\mathbf{x}) + \dddot{x}_d - 2\lambda\ddot{\tilde{x}} - \lambda^2\dot{\tilde{x}}\right) - K_{SM}sat(s/\phi) \tag{14}$$

which, with $s = \ddot{\tilde{x}} + 2\lambda\dot{\tilde{x}} + \lambda^2\tilde{x}\cdot\hat{f}(\mathbf{x})$ and $\hat{b}(\mathbf{x})$ are the best estimates of the functions in model (13), considering the approximate values for the parameters, the measured mass position (x), estimated velocity ($\dot{x}$) and acceleration ($\ddot{x}$) and the estimate of the variable ξ given in (12). Low pass filter is used to obtain the velocity and acceleration from the measured position (x). x_d is the desired position of the actuator load (set-point), λ is a positive constant related to the cut-off frequency of the closed-loop system, ϕ is the boundary layer thickness necessary to avoid control chattering, and K_{SM} is a control gain related to the modeling and parameter estimation errors.

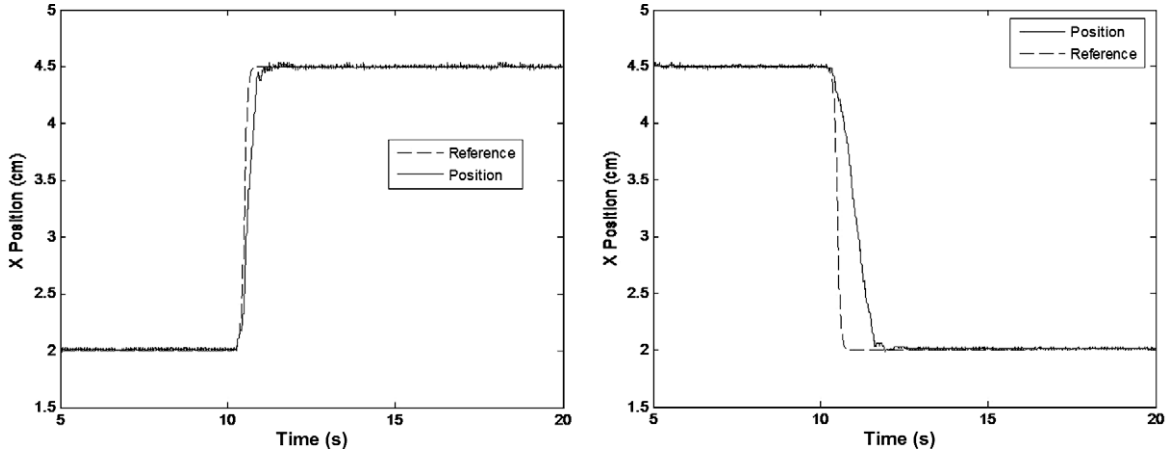

Fig. 13. Step responses of the SMA actuator (left – positive; right – negative).

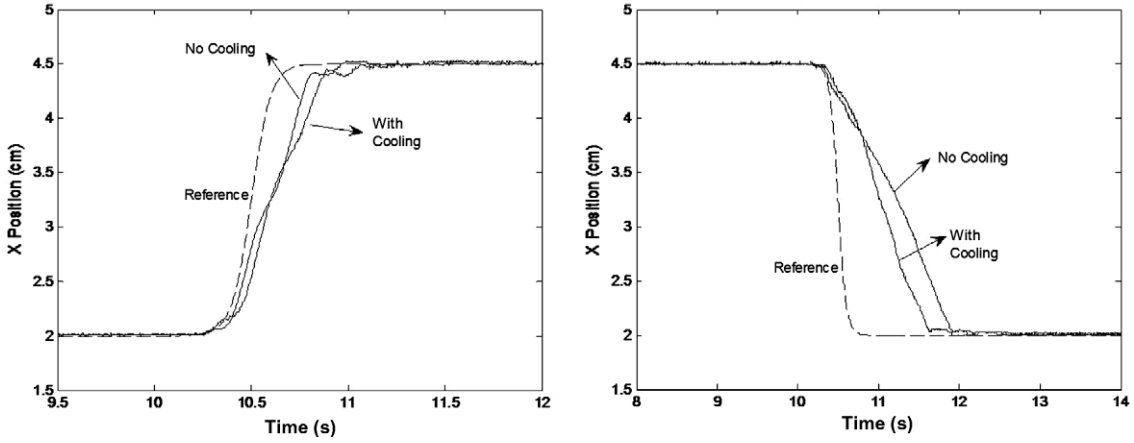

Fig. 14. Step response of the SMA actuator. Effect of cooling (left – positive; right – negative).

A detailed description of the control design may be found in Slotine and Li [16].

5. Experimental results

The control logic previously developed was applied to the experimental prototype, and the performance of the closed-loop system was be evaluated. Fig. 13 shows a reference step of 2.5 cm applied at $t = 10$ s, for both positive and negative step responses. Control parameters are $\lambda = 40$; $\phi = 1.6$ and $K_{SM} = 64$. The 5% settling time obtained for the positive step response is 0.23 s, and the maximum overshoot is 0.6%. For the negative step response, the settling time is 0.92 s, with no overshoot. It must be stressed that the cooling performance is worse than the heating one, even with the proposed cooling system. Such behavior is evidence of the necessity of a cooling system. The same experiment was carried out without the cooling system, and the results are presented in the Fig. 14 and in Table 1. For this case, control parameters were adjusted to $\lambda = 50$; $\phi = 2$, and $K_{SM} = 100$, after a tuning procedure. Without cooling, the heating performance is better; however, the cooling is even slower.

Table 1
Effect of cooling system in the step response.

	No cooling (s)	With cooling (s)
Settling time-up	0.16	0.22
Settling time-down	1.20	0.92

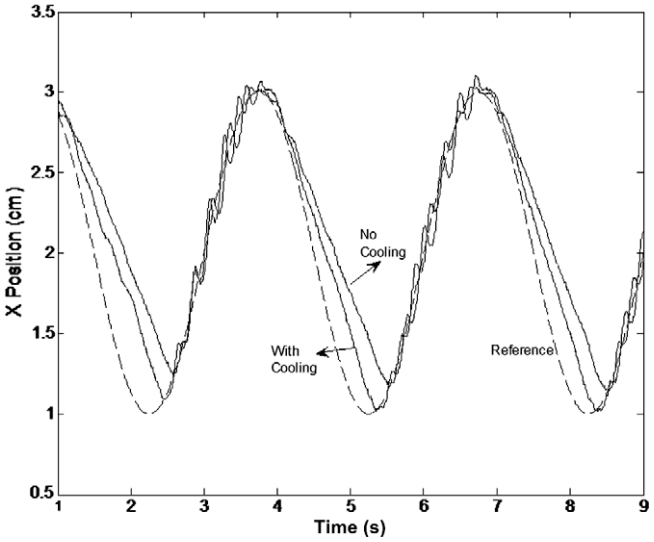

Fig. 16. Harmonic set-point response of the SMA actuator (1 cm amplitude), 3 s period, with and without cooling.

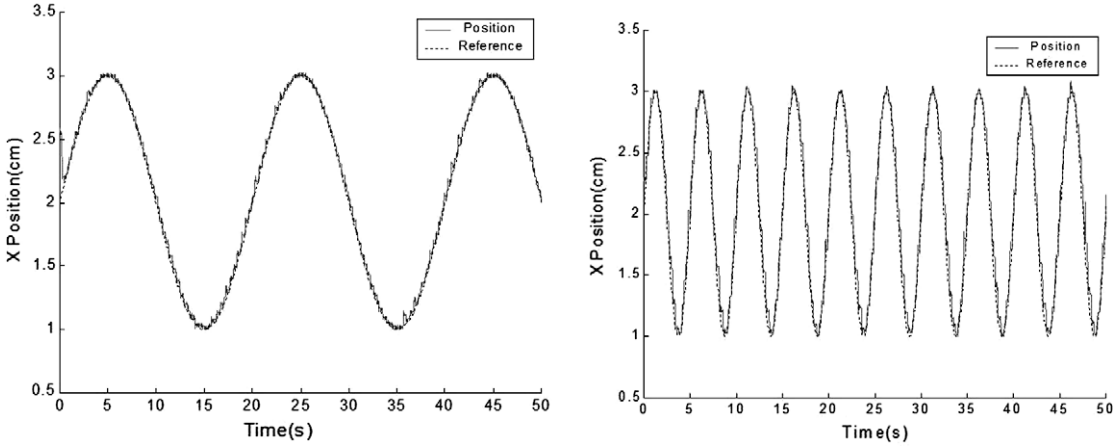

Fig. 15. Harmonic set-point response of the SMA actuator (1 cm amplitude). (Left) 20 s period; (Right) 5 s period.

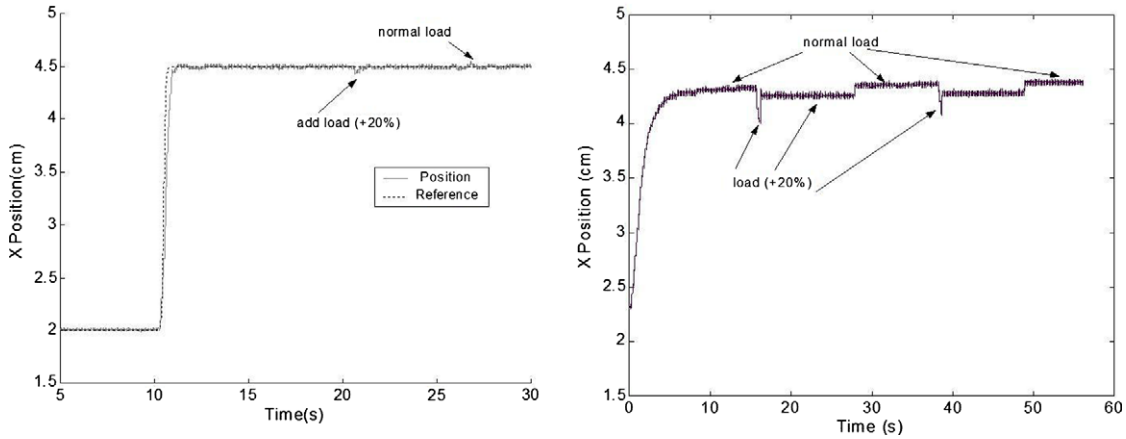

Fig. 17. Load disturb (±20%) response of the SMA actuator (left) closed-loop; (right) opened- loop.

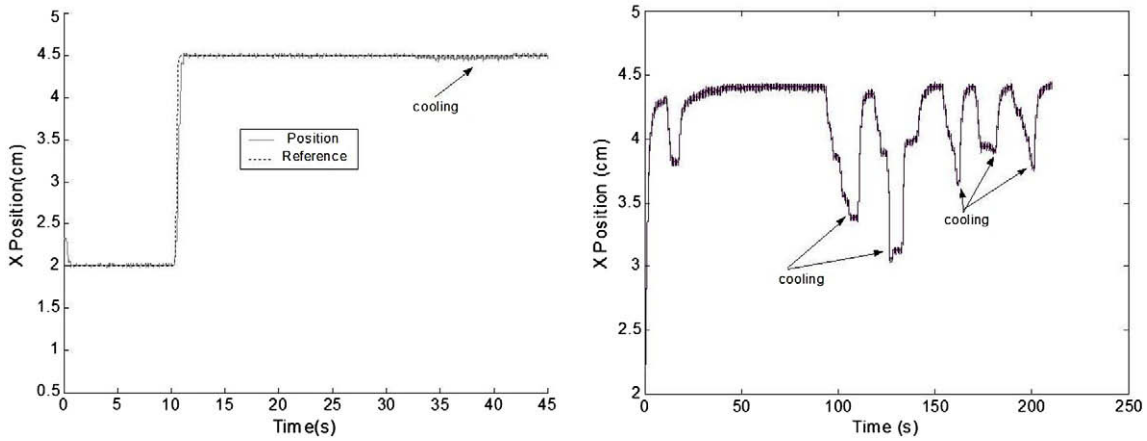

Fig. 18. Cooling disturb response of the SMA actuator (left) closed-loop; (right) opened-loop.

A harmonic set-point was applied to the actuator, with amplitude of 1 cm and periods of 20 s and 5 s (Fig. 15). It can be seen that, despite a small oscillation around the set-point, the system follows the reference with good accuracy. Tests with decreasing periods indicated a 0.69 Hz cut-off frequency, despite a value of 0.37 Hz obtained with a conventional PID controller.

The harmonic set-point was also applied to the actuator without the cooling system, with a period of 3 s. Fig. 16 shows that during the cooling phase, the actuator is not able to follow the reference, with even worse behavior in the absence of a cooling system. A cut-off frequency of 0.52 Hz was obtained for the actuator without the cooling system, using the sliding mode controller.

This figure illustrates the necessity of the cooling system in order to increase the frequency response of SMA actuators, since the heating process is very fast and is not a limiting factor in the frequency response. The main objective of the thermoelectric cooling system is to "equalize" the cooling time to the heating time, in order to obtain a better frequency response of the actuator.

Finally, a load disturbance was applied, equivalent to ±20% in the load mass (Fig. 17), as well as a cooling disturbance (Fig. 18), created by a computer cooler fan directed toward the SMA wire. The robustness of the controller in a closed-loop system (left plots) may be compared with an open-loop (right plots). The magnitude of the disturbance, and its effect in the actuator, may be qualitatively evaluated by the open loop response.

6. Conclusions

A novel SMA actuator was proposed, using the thermoelectric effect, for cooling the SMA wire. An experimental prototype was built, and a mathematical model was developed. The model parameters were adjusted by means of an experimental identification procedure. The validated model was then used to design a sliding mode controller. Such a controller is able to deal with model and parameter uncertainties, and also with non-linear effects. Closed-loop preliminary results obtained in the experimental setup showed that the proposed actuator presents a good dynamic response and low sensibility to disturbances of load and ambient cooling. Therefore, it is recommended for applications with SMA devices.

Acknowledgements

This work has been supported by the Brazilian National Research Council (CNPq), process number 484232/2006-1. The second author also acknowledges the CNPq research grant 301686/2007-6.

References

[1] Abadie J, Chaillet N, Lexcellent C. An integrated shape memory alloy microactuator controlled by thermoelectric effect. Sensor Actuator A 2002;99:297–303.

[2] Asada HH, Mascaro S. Wet Shape Memory Alloy Actuators, MIT Home Automation and Healthcare Consortium, Phase 3 Final Report, Boston, USA, 2002.
[3] Bhattacharyya A, Lagoudas D, Wang Y, Kinra K. On the role of thermoelectric heat transfer in the design of SMA actuators: Theoretical modeling and experiment. Smart Mater. Struct. 1995;4:252–63.
[4] Ding Z, Lagoudas DC. Solution behavior of the transient heat transfer problem in thermoelectric shape memory alloy actuators. SIAM J. Appl. Math. 1997;57(1):34–52.
[5] Dutta SM, Ghorbel FH. Differential hysteresis modeling of a shape memory alloy wire actuator. IEEE/ASME Trans. Mech. 2005;10(2):189–97.
[6] Dynalloy Inc., Flexinol – Wire specifications. 2005. <http://www.dynalloy.com>; 2005 [accessed 20.12.05].
[7] Elahinia HM, Ashrafiuon H. Nonlinear control of a shape memory alloy actuated manipulator. ASME J. Vib. Acoust. 2002;124:566–75.
[8] Furuya Y, Shimada H. Shape memory actuator for robotic applications, engineering aspect of shape memory alloys. London: Butterworth-Heinemann; 1990. p. 338–55.
[9] Gorbet BR, Russel AR. Improve the response of SMA actuators. In: IEEE international conference on robotic and automation, vol. 3; 1995, p. 2299–303.
[10] Grant D, Hayward V, Lu A. Design and comparison of high strain shape memory alloy actuators. In: International conference on robotic and automation, Albuquerque, New Mexico; 1997. p. 260–5.
[11] Hoder K, Vasina M, Solc F. Shape memory alloy – unconventional actuators. In: International conference on industrial technology ICIT, Maribor, Slovenia; 2003. p. 190–3.
[12] Ikuta K, Tsukamoto M, Hirose S. Mathematical model and experimental verification of shape memory alloy for designing micro actuator. In: Proceedings of the IEEE on micro electromechanical systems, an investigation of microstructures, sensors, actuators, machines, and robots; 1991. p. 103-8.
[13] Incropera PF, Witt DPD. Fundamentos de transferência de calor e de massa, 4th ed., Rio de Janeiro, LTC; 1998 [in Portuguese].
[14] Khan M, Lagoudas D, Rediniotis O. Thermoelectric SMA actuator: Preliminary prototype testing. In: Proceedings of SPIE smart structures and materials, vol. 5054; 2003. p. 147-155. .
[15] Semenyuk V, Seelecke S, Stockholm J, Musolff A. The use of thermoelectric cooling for shape memory wire temperature control. In: Proceedings of ECT '98; 1998.
[16] Slotine JJE, Li W. Applied nonlinear control. Englewood Cliffs, USA: Prentice-Hall; 1991.
[17] Tanaka Y, Yamada Y. A rotary actuator using shape memory alloy for a robot, and analysis of the response with load. In: IEEE/RSJ International workshop on intelligent robots and systems IROS'91, Osaka, Japan; 1991. p. 1163–8.